Statistical multipoles for cusp electrons and Rydberg electrons

Joachim Burgdörfer
University of Tennessee, Knoxville, Tennessee 37996
and Oak Ridge National Laboratory, Oak Ridge, Tennessee 37831
(Received 16 September 1985)

A unified description for anisotropic near-threshold excitation in terms of statistical O(4) multipoles is presented. It is shown that a single set of multipole parameters can characterize both the angular distribution of low-energy electron emission and the nonstatistical population of high Rydberg states. Relations between multipole moments of the bound-state charge cloud and of multipole moments of the velocity distributions are derived. The formalism is applied to electron capture to the continuum and into Rydberg states for $H^+ + He$ using the continuum distorted-wave approximation. Comparison is made with recent experimental data.

I. INTRODUCTION

Cross sections for electron emission in inelastic ion-atom collisions show a strong enhancement at electron velocities $\mathbf{v}_e$ approximately equal to the projectile velocity $\mathbf{v}_p$. This gives rise to a cusp[1,2] in the experimentally observed doubly differential cross section (DDCS) $d\sigma/d\mathbf{v}_e$. Two different processes contribute to the cusp: target ionization [i.e., electron capture to continuum (ECC)] and projectile ionization [i.e., electron loss to continuum (ELC)]. In both cases, the final electron states lie in the low-energy continuum ($v \to 0$) of the projectile, where $\mathbf{v} = \mathbf{v}_e - \mathbf{v}_p$ denotes the electron velocity in the rest frame of the projectile.

A theoretical explanation for the occurrence of a cusp was first given by Macek and Rudd,[3,4] who pointed out that ECC can be visualized as a smooth continuation across the ionization limit of capture into excited bound states with increasingly larger orbits such that the captured electron finally becomes unbound.

Recent experiments and theories for both ECC and ELC show a large variety of anisotropies and asymmetries to be present in DDCS. A detailed analysis of nonisotropic structures has become feasible since recent experimental advances permit measurements of the two-dimensional electron distribution.[5,6] Concurrently, the formation of Rydberg states in ion-atom and ion-solid collision has gained considerable interest. Recent experiments[7-9] provided clear evidence for a nonstatistical and partially coherent population of high n levels.

It is intuitively clear that the population of low-lying continuum states and high-lying Rydberg states should be strongly related to one another (Fig. 1). The transition amplitude $t_{i,f}$ for capture (or excitation) of an electron from a deeply bound initial state (i) into highly excited final state (f) is expected to be a smooth function of f as the ionization threshold is crossed since this amounts only to a slight change in the electronic energy transfer ($\Delta\varepsilon$) during the collision.

The goal of this paper is to establish a direct quantitative relationship between anisotropy parameters characterizing the nonstatistical coherent excitation above threshold (cusp electrons) and those characterizing similar excitation processes of manifolds just below the ionization threshold (Rydberg electrons).

The Coulombic final-state interaction between the projectile ion and the ejected electron plays a decisive role not only for the occurrence of the cusp but also for the anisotropy of near-threshold excitation. According to Wigner's threshold law[10] all partial waves are present in the zero-velocity ($v \to 0$) continuum at threshold in the specific case of an attractive Coulomb field unlike the case of final-state interactions of short range. The cusp anisotropy may be described in terms of the partial-wave populations and of coherences between different partial waves. Our analysis employs therefore the dynamical O(4) symmetry group of the Coulomb problem. It will be shown that a set of O(4) multipoles originally[11] introduced to classify bound-state coherences is well suited to also describe continuum-state coherences. The anisotropy parameters in the DDCS for electron emission can be ex-

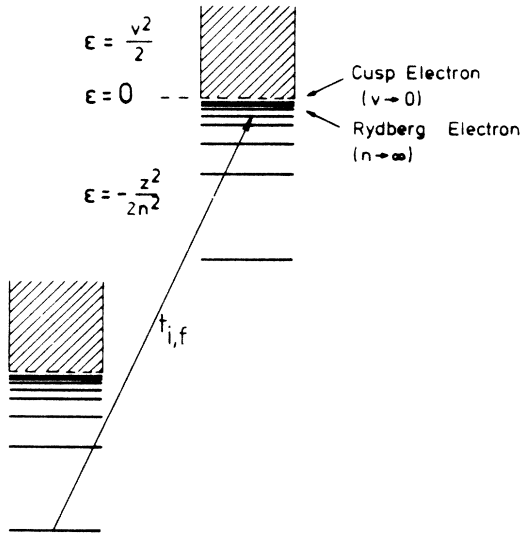

FIG. 1. Energy-level diagram for electron capture as seen in the target frame.

pressed as expectation values of O(4) multipoles.

The plan of the paper is as follows. In Sec. II we briefly review the density-matrix description of bound-state coherences in terms of expectation values of O(4) operators. Their Rydberg limit and the connection with the orbital parameter of Kepler orbits is investigated in Sec. III. In Sec. IV we relate the multipole expansion for cusp electron emission[12] devised by Meckbach, Nemirovsky, and Garibotti with multipoles for coherent Rydberg excitation and derive explicit formulas to express the cusp cross section in terms of coherent continuum and bound-state excitation [Eqs. (36) and (40)].

The present method facilitates the theoretical determination of anisotropy parameters for excitation into the continuum by smoothly extrapolating equivalent bound-state excitation parameters across the threshold. As an illustrative example, we will study in Sec. V the ECC process $H^+ + H \rightarrow H(n) + H$ in detail using the continuum distorted-wave[13] (CDW) approximation. The present approach permits also direct quantitative comparison of seeminly different data such as extracted from electron emission studies and from photon emission studies, elucidating thereby the common underlying physics. As an example we analyze experimental data for charge transfer $H^+ + He \rightarrow H(n) + He^+$ in Sec. VI. Atomic units are used unless otherwise stated.

II. DENSITY-MATRIX DESCRIPTION FOR BOUND-STATE EXCITATION

Due to the nonadiabatic nature of inelastic ion-atom collisions the final electronic state is, in general, a coherent mixture of atomic substates. The coherent excitation is most completely described by the density matrix[14] which contains an ensemble average over all unresolved degrees of freedom in a given scattering process. If, for example, the scattering angle of the outgoing projectile is not detected, the density matrix is given in terms of the transition amplitudes, $t_{i,nlm}(\mathbf{K})$, by

$$\langle nlm \mid \sigma \mid nl'm' \rangle = \frac{\delta_{m,m'}}{(2\pi)^2 v_p} \int d^3K \, t^*_{i,nl'm'}(\mathbf{K}) t_{i,nlm}(\mathbf{K}) \times \delta(\mathbf{K}\cdot\mathbf{v}_p + \Delta\varepsilon) \, . \quad (1)$$

The momentum transfer during the collision is denoted by $\mathbf{K}$ and $\Delta\varepsilon$ is the change in the electronic energy. The density matrix is diagonal in m because the momentum transfer integral (1) extends over all scattering angles. Notice that the quantization axis is chosen along the axis of the incident beam. The density matrix is, however, nondiagonal with respect to l. Equation (1) contains the maximum information on the collision amplitudes available in an angle-integrated experiment. The usual substate cross sections corresponding to diagonal elements in (1), on the other hand, do not completely specify the final-state population. Off-diagonal elements of (1) describing coherences between different substates are observable only for (nearly) degenerate manifolds. For larger energy splittings and experimentally limited time resolution the average over rapid phase oscillations due to the time evolution under the influence of the *isolated atomic Hamiltonian,*

$$\langle f \mid \sigma(t) \mid f' \rangle = \exp[it(\varepsilon'_f - \varepsilon_f)] \langle f \mid \sigma(0) \mid f' \rangle \, , \quad (2)$$

extinguishes final-state coherences in the ensemble. Angular momentum coherences will play a crucial role for an understanding of anisotropies in the low-energy continuum.

As the number of nonvanishing off-diagonal elements in an angle-integral measurement rapidly increases in a Rydberg series like $\sim n^3$, the problem of finding a convenient and physically sensible basis in the Liouville space of density-matrix elements arises. In general, a basis consists of set operators $\{O_i\}_{i \geq 1}$ whose expectation values $\mathrm{Tr}(\sigma O_i)/\mathrm{Tr}\sigma$ parametrize the density matrix for a given manifold. Apart from the requirement for the operator set to form a complete basis with respect to the manifold under consideration, one has a wide freedom in selecting an appropriate operator set. For example, the operators O_i need not commute with the Hamiltonian of the observed atomic subsystem. One may seek a convenient representation that allows an expansion of the density operator in terms of only a few, physically meaningful expectation values. It is clear that the actual choice depends on the underlying excitation mechanism. For example, a standard basis in Liouville space, the operator set $\{ \mid nlm \rangle \langle n'l'n' \mid \}$, whose expectation values are just the density-matrix elements in the standard basis [Eq. (1)], is certainly complete with respect to an n manifold. However, it does not provide a simple and transparent representation of the density operator when many different $\mid lm \rangle$ states are coherently populated in the collision process.

A well-suited representation taking explicitly into account the l mixing in (nearly) degenerate manifolds can be found by exploiting the dynamical O(4) symmetry ("supersymmetry") of the Coulomb problem. The O(4) symmetry is related to the existence of two constants of motion, the angular momentum $\mathbf{L}$ and the Runge-Lenz vector $\mathbf{A}$,

$$\mathbf{A} = \tfrac{1}{2}(\mathbf{p}\times\mathbf{L} - \mathbf{L}\times\mathbf{p}) - Z_p \frac{\mathbf{r}}{r} \, . \quad (3)$$

In a classical picture, $\mathbf{A}$ points from the nucleus to the "perihelion" of the electron orbit and defines its principal axis (see Fig. 2). $\mid \mathbf{A} \mid$ is proportional to the eccentricity ε of the orbit ($\mid \mathbf{A} \mid = Z_p \varepsilon$, where we have approximated the reduced mass of the electron by unity). It can be shown[11] that the two generators of the dynamical symmetry group, $\mathbf{L}$ and $\mathbf{A}$, give rise to a complete set of multipole operators whose expectation values provide a unique parametrization of the density matrix for a given n shell. This particular choice has several decisive advantages: all basis elements are constants of motion of the atomic Hamiltonian (or approximate constants of motion when relativistic corrections are taken into account) and are directly related to the (quasi)degeneracy [Eq. (2)] which, in turn, is a prerequisite for an experimental observation of coherences; their expectation values have a simple physical interpretation; all relevant matrix elements can be simply expressed in terms of angular momentum coupling coefficients; and this representation provides a direct decompo-

sition of the density operators into different components according to their tensorial rank, parity, and time-reversal symmetry. The latter is of particular importance when the collision process leads to a selective excitation of a certain subspace of the Liouville space (for example, predominantly low-order multipoles). In Sec. III we will discuss one example in more detail.

The density operator can be expanded in terms of a basis set of spherical statistical O(4) multipoles,[11]

$$\sigma=\sum_{\substack{\Pi,k,k_1,k_2\\ k_1\geq k_2}}\sigma_0^k(\Pi,k_1,k_2)[U_0^k(\Pi,k_1,k_2)]^\dagger , \tag{4}$$

where

$$\sigma_q^k(\Pi,k_1,k_2)=\mathrm{Tr}[\sigma U_q^k(\Pi,k_1,k_2)] . \tag{5}$$

For the sake of simplicity, we have restricted the multipole expansion in (4) to spherical components with $q=0$ in accordance with the axially symmetric density matrix ($\delta_{m,m}$) in an angle-integral density matrix. The quantum number $\Pi=0$ (1) characterizes the even (odd) parity of the statistical multipole. A generalization to $q\neq 0$ is straight forward.[11] The operators U^k in (4) are defined as

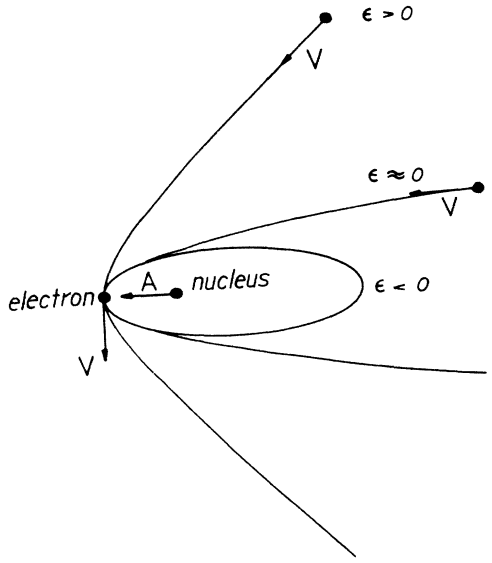

FIG. 2. Classical orbits for the Coulomb problem. States near threshold ($\varepsilon=0$) correspond to parabolas. At large distances from the nucleus **v** becomes (anti)parallel to **A**.

$$U_{q=0}^k(\Pi,k_1,k_2)=\frac{i^{k_1+k_2-k}[(2k_1+1)(2k_2+1)]^{1/2}}{[2(1+\delta_{k_1,k_2})]^{1/2}\langle j||j^{k_1}||j\rangle\langle j||j^{k_2}||j\rangle}$$

$$\times\sum_{q_1,q_2}\langle k_1k_2q_1q_2\,|\,k0\rangle[(j^{(1)})_{q_1}^{k_1}(j^{(2)})_{q_2}^{k_2}+(-1)^\Pi(j^{(2)})_{q_1}^{k_1}(j^{(1)})_{q_2}^{k_2}] \tag{6}$$

in terms of two commuting pseudospin operators $\mathbf{j}^{(1,2)}$. The latter are given in terms of **L** and the normalized Runge-Lenz (RL) vector $\mathbf{a}=(n/Z_P)\mathbf{A}$ by

$$\mathbf{j}^{(1,2)}=\tfrac{1}{2}(\mathbf{L}\mp\mathbf{a}) . \tag{7}$$

In (6), $\langle j||j^{k_i}||j\rangle$ denotes the reduced matrix element of the spherical multipole of rank k for the pseudospin operator $j^{(i)}$ and

$$2j+1=n . \tag{8}$$

With use of the fact that **L** is odd and **A** is even under time reversal, it can be shown[11] that U^k has a well-defined time-reversal quantum number

$$t=(-1)^{k_1+k_2+\Pi} . \tag{9}$$

The set (6) forms an orthonormal basis set in the sense of the trace metric in the Liouville space,[15,16]

$$\mathrm{Tr}[U_q^k(\Pi,k_1,k_2)^\dagger U_{q'}^{k'}(\Pi',k_1',k_2')]=\delta_{k,k'}\delta_{q,q'}\delta_{\Pi,\Pi'}\delta_{k_1,k_1'}\delta_{k_2,k_2'} . \tag{10}$$

Finally, the expectation values of O(4) multipoles can be related to the density-matrix elements in the standard basis with the help of some straightforward angular momentum algebra:[11]

$$\sigma_0^k(n,\Pi,k_1,k_2)=\frac{i^{k_1+k_2-k}}{[2(1+\delta_{k_1,k_2})]^{1/2}}\sum_{l,l'=0}^{n-1}[(2k_1+1)(2k_2+1)(2_l+1)(2l'+1)]^{1/2}[(-1)^\Pi+(-1)^{l+l'}]\begin{Bmatrix} j & j & k_1\\ j & j & k_2\\ l & l' & k\end{Bmatrix}\rho_q^k(l,l')^* \tag{11}$$

with

$$\rho_q^k(l,l')=\sum_{m,m'}(-1)^{l-m}\sqrt{2k+1}\begin{pmatrix} l & k & l' \\ -m & q & m' \end{pmatrix} \times\langle nlm\,|\,\sigma\,|\,nl'm'\rangle\ . \tag{12}$$

The usual state multipoles[14] are denoted by ρ_q^k. Since we will later study the limit $n\to\infty$ of (11) in detail, we have explicitly displayed the n dependence of σ_0^k. As we will discuss in subsequent sections, the decisive advantage of the O(4) basis set is to clearly exhibit the physical meaning of coherence parameters by relating them to orbital parameters such as $\langle A_z\rangle$ that have a simple classical analog for Kepler orbits.

III. RYDBERG LIMIT OF BOUND-STATE MULTIPOLES

The set of statistical multipoles, Eq. (11), is expected to be particularly useful for highly excited n manifolds. While the number of density-matrix elements $\langle nlm\,|\,\sigma\,|\,nl'm\rangle$ increases dramatically as $n\to\infty$ and a determination of all individual matrix elements becomes, theoretically as well as experimentally, a formidable task, a few statistical multipoles should provide an adequate description of the most important and characteristic features of the shape of the coherently excited charge cloud. This conjecture is supported by a classical orbital picture that should become increasingly valid as n tends to infinity (more precisely, as $n,l\to\infty$). In the classical limit, a few orbital parameters suffice to characterize the Kepler orbit completely.

We explore this conjecture by studying the Rydberg limit of the O(4) multipoles. In Eqs. (11) and (12) both the density-matrix elements $\langle nlm\,|\,\sigma\,|\,nl'm\rangle$ and the expansion coefficients [through $j=(n-1)/2$ in the $9j$ symbol] are n dependent. While the $n\to\infty$ limit in the density-matrix elements depends on the excitation mechanism under consideration, the expansion of O(4) multipoles in terms of standard density-matrix elements can be drastically simplified in the limit $j\to\infty$ ($n\to\infty$) under the assumption

$$l,l'\ll j\ , \tag{13}$$

i.e., that only a narrow band of low final l states significantly contributes. For most of the collisional excitation mechanisms known to date[17] (direct excitation, electron capture, and ion-solid interaction), population of l values is restricted to[8] $l\lesssim 20$, and Eq. (13) is certainly satisfied for high n states (say, $n\gtrsim 100$).

In the limit $j\to\infty$ ($n\to\infty$) we find[18]

$$\begin{Bmatrix} j & j & k_1 \\ j & j & k_2 \\ l & l' & k \end{Bmatrix}=\frac{(-1)^{l'+k_2}}{2j+1}\begin{pmatrix} l & l' & k \\ 0 & 0 & 0 \end{pmatrix}\begin{pmatrix} k_1 & k_2 & k \\ 0 & 0 & 0 \end{pmatrix}+O(1/j^2)\ \text{ as } j\to\infty\ . \tag{14}$$

The statistical multipoles are then given by

$$\sigma_0^k(n,\Pi,k_1,k_2)=\frac{i^{k_1+k_2-k}}{(1+\delta_{k_1k_2})^{1/2}}(-1)^{k_2}[(2k_1+1)(2k_2+1)]^{1/2}\begin{pmatrix} k_1 & k & k_2 \\ 0 & 0 & 0 \end{pmatrix} \times\sum_{l,l'=0}^{\infty}(-1)^{l'}\sqrt{(2l+1)(2l'+1)}\begin{pmatrix} l & k & l' \\ 0 & 0 & 0 \end{pmatrix}[(-1)^{\Pi}+(-1)^{l+l'}][\rho_0^k(l,l')]^*\ , \tag{15}$$

where ρ_0^k denotes now the Rydberg limit of Eq. (12) to be discussed in Sec. V for the specific case of an electron capture process. The $3j$ symbols in (15) lead to a drastic reduction of the number of contributing multipoles. σ_0^k is nonzero only if

$$l+l'+\Pi=\text{even}\ , \tag{16a}$$

$$l+l'+k=\text{even}\ , \tag{16b}$$

and

$$k_1+k_2+k=\text{even}\ . \tag{16c}$$

Equation (16a) reflects the well-known fact that multipoles of odd parity require angular momentum coherences of odd parity (i.e., $l+l'$ odd, for example, s-p coherence). Combining (16a) and (16b) we have $\Pi+k=$even, i.e., multipoles of even (odd) rank possess even (odd) parity. Finally, with the help of (16c) we find

$$k_1+k_2+\Pi=\text{even}\ . \tag{16d}$$

In view of Eq. (9) this implies that only multipoles even under time reversal contribute in the Rydberg limit to leading order. The Rydberg limit of (11) projects the complete density matrix onto the Liouville subspace defined by the selection rules [Eq. (16)]. This part of the density matrix is expected to be most important for near-threshold excitation. The occurrence of selection rules can be understood by considering the Rydberg limit of the pseudospin operators [Eq. (7)]:

$$\frac{\mathbf{j}^{(1,2)}}{n}=\frac{1}{2}\left[\mp\frac{\mathbf{A}}{Z_P}+\frac{\mathbf{L}}{n}\right]. \tag{17}$$

As $n\to\infty$, the eigenvalues of $\mathbf{A}/Z_P$ (the eccentricity) and of $\mathbf{j}^{(1,2)}/n$ approach finite values while $\mathbf{L}/n$ tends to zero since the l values are restricted to a finite range [Eq. (13)], and consequently

$$\lim_{n\to\infty}\mathbf{j}^{(1,2)}/n=\mp\frac{1}{2Z_P}\mathbf{A}. \tag{18}$$

The two pseudospins are no longer independent of each other but become directly proportional to the Runge-Lenz (RL) vector itself. Equation (18) also gives rise to the linear dependence in Eq. (15) of all σ_0^k with different (k_1,k_2) but equal k. We note that the selection rules (16) are one important example for the above-mentioned reduction of the density operator when the underlying excitation mechanism displays a certain selectivity. In this case the relatively weak assumption about the population of only low and intermediate l states [Eq. (13)] leads to a drastic restriction of the density operator to a subspace of the Liouville space which is spanned up by multipoles of the Runge-Lenz vector alone. While alternative choices for a basis are certainly possible, this fact underlines the particular convenience of the O(4) basis.

Without loss of generality one may choose for simplicity $k_2=0$ in Eq. (15) and the final expression for statistical multipoles in the Rydberg limit then reads

$$\sigma_0^k(n,\Pi,k,0)=\frac{(-1)^k}{n}(2-\delta_{k,0})^{1/2}\sum_{l,l'=0}^{\infty}(-1)^l\sqrt{(2l+1)(2l'+1)}\begin{pmatrix}l & k & l'\\ 0 & 0 & 0\end{pmatrix}\rho_0^k(l,l')\ \text{ as } n\to\infty\ . \tag{19}$$

The equivalence of the pseudospins and the RL vector in the Rydberg limit [Eq. (18)] furthermore permits an interpretation of the statistical multipoles [Eq. (19)] in terms of multipoles of the Runge-Lenz vector. Using (6) and explicit expressions for reduced matrix elements,[19] one can find

$$U_0^k(\Pi,k,0)=\left[-\frac{n}{Z_P}\right]^k\left[\frac{(2-\delta_{k,0})(2k+1)(n-k-1)!}{n[(n+k)!]}\right]^{1/2}A_0^k\ \text{ as } n\to\infty\ . \tag{20}$$

For later reference we note that for $k=1$, Eq. (20) is exact for all n. Expectation values of the RL vector can be deduced from the unnormalized density matrix as

$$\langle A_0^k\rangle=\mathrm{Tr}(\sigma A_0^k)/\mathrm{Tr}\sigma\ . \tag{21}$$

The statistical multipoles and the expectation value of the RL operator are therefore related to each other by

$$\sigma_0^k(n,\Pi,k,0)/\sigma_0^0(n,0,0,0)=\left[\frac{-1}{Z_P}\right]^k[(2k+1)(2-\delta_{k,0})]^{1/2}\langle A_0^k\rangle\ \text{ as } n\to\infty\ , \tag{22}$$

where we have used that

$$\sigma_0^0(n,0,0,0)=\frac{1}{n}\sum_{l,m}\langle nlm\mid\sigma\mid nlm\rangle=\mathrm{Tr}\sigma/n\ . \tag{23}$$

Equation (22) determines multipoles of the RL vector in a Rydberg manifold. The latter correspond to the dipole moment, quadrupole moment, etc. of the *charge cloud* of a Rydberg electron. It should be noted that the usual Fano-Macek alignment parameters[20] (for example, $\langle L_0^2\rangle$) do *not* give direct information on the alignment of the charge cloud in the l-mixing regime but describe the alignment parameters of the *angular momentum vector* which are, in general, statistically independent observables.

IV. MULTIPOLE EXPANSION OF THE CUSP ELECTRON DISTRIBUTION

Meckbach, Nemirovski, and Garibotti[12] have devised a double series expansion of the doubly differential cross section (DDCS) for emission of low-energy electrons that has proven to be very useful for an apparatus-independent analysis and presentation of the experimental cusp data. In the projectile rest frame the DDCS is expanded as

$$\frac{d\sigma}{d\mathbf{v}}=\frac{1}{v}\sum_{i=0}^{\infty}\sum_{k=0}^{\infty}B_i^k v^i P_k(\cos\theta)\ , \tag{24}$$

where v is the radial velocity of the electron and θ the polar angle of emission. A cusp shape is uniquely characterized by a set of expansion coefficients B_i^k. For low-energy electrons ($v\to 0$) only a few terms ($i=0,1,2,\ldots$) in the radial expansion contribute. The leading term ($i=0$) provides the well-known cusp singularity ($\sim 1/v$).

We restrict ourselves in the following theoretical analysis as well as in the comparison with data to the leading multipoles of the angular distribution ($\sim B_0^k$). These terms clearly dominate the cross section at threshold and are the ones that possess a direct connection with bound-state multipoles. There is, in addition, a conceptual difficulty that makes a meaningful comparison between experiment and theory questionable for higher-order terms ($\sim B_i^k$, $i\geq 1$) in the expansion (24). To illustrate

this point we consider the first-order Faddeev expansion[3,21] for electron capture to continuum. As first poined out by Macek[3] the transition amplitude can be written as a coherent superposition of a direct ionization amplitude, $t^I_{i,\mathbf{v}_e}$ (with a target-centered continuum final state), of a genuine ECC amplitude, $t^{\mathrm{ECC}}_{i,\mathbf{v}}$ (with a projectile-centered continuum final state) and of a plane-wave counter term, $t^{\mathrm{PW}}_{i,\mathbf{v}_e}$, as

$$t_{i,\mathbf{v}_e}=t^I_{i,\mathbf{v}_e}-t^{\mathrm{PW}}_{i,\mathbf{v}_e}+t^{\mathrm{ECC}}_{i,\mathbf{v}} . \tag{25}$$

Neglecting, for the moment, (Coulomb) phase factors, the amplitudes t^I and t^{PW} are expected to be smooth functions of v_e at large v_e in the vicinity $\mathbf{v}_e\cong\mathbf{v}_p$, allowing for a Taylor expansion in $v=|\mathbf{v}_e-\mathbf{v}_p|$. The amplitude t^{ECC}, on the other hand, possesses an algebraic singularity $v^{-1/2}$ originating from the normalization of the continuum wave function.[22] Therefore, the v expansion of the transition probability, and hence the cross section, reads

$$|t_{i,\mathbf{v}_e}|^2=\frac{a_0}{v}+\frac{a_1}{v^{1/2}}+a_2+a_3v^{1/2}+\cdots . \tag{26}$$

Equation (26) contains terms with algebraic singularities at threshold $\sim v^{n/2}$, $n=-1,1,3,\ldots$, not included in the expansion (24). The latter represent interference terms between an ECC process and direct ionization. Determination of all higher-order coefficients is equivalent to a proper treatment of the so-called "background" which is, in fact, an integral part of the ionization process.[2] The fitted values for higher-order terms B^k_i ($i\geqq 1$) in Eq. (24) may therefore be distorted by the lack of additional interference terms in the expansion. The leading term with the strongest singularity (v^{-1}), on the other hand, should be basically unaffected. It represents the genuine ECC or ELC process and is independent of interferences between different partial amplitudes [Eq. (25)] in the Faddeev expansion. We note that taking into account Coulomb phases, one may expect in addition terms $\sim\log_e(v)$ in the expansion (26). Since relative phases of partial amplitudes are generally only poorly represented by low-order Faddeev approximations,[3,21] a reliable calculation of correction terms in the v expansion is difficult. This problem can be circumvented rather than solved by restricting to the physically most important singular part from the onset.

The genuine ($v\to 0$) DDCS for ELC or ECC can be expressed in terms of the isotropic cross section σ_0 and the anisotropy coefficients β_k as

$$\frac{d\sigma}{d\mathbf{v}}=\frac{\sigma_0}{v}\sum_{k=0}^{\infty}\beta_kP_k(\cos\theta) , \tag{27}$$

where

$$\sigma_0=B^0_0v \tag{28a}$$

and

$$\beta_k=B^k_0/B^0_0 . \tag{28b}$$

Pursuing the idea of continuity of all excitation parameters across the ionization limit,[3] we relate the expansion coefficients (28) with the statistical O(4) multipoles for Rydberg excitation. To this end we first expand the DDCS in terms of the density matrix for coherent partial-wave excitation in the continuum. Using a partial-wave expansion of the wave function, one finds to leading order $v^{-1/2}$,

$$\psi^{\pm}_{\mathbf{v}}(\mathbf{r})=e^{\pm i\gamma}\sum_l(-1)^{(l/2)(1\mp1)}\psi_{vlm}(\mathbf{r})[Y^m_l(\hat{\mathbf{v}})]^* , \tag{29a}$$

$$\psi_{vlm}(\mathbf{r})=\left[\frac{2}{rv}\right]^{1/2}J_{2l+1}[(8Z_Pr)^{1/2}]Y^m_l(\hat{\mathbf{r}}) , \tag{29b}$$

where $+$ ($-$) denotes the outgoing (incoming) Coulomb wave, J_k is the Bessel function, and Z_P denotes the charge of the projectile. γ denotes a divergent but (l,m)-independent Coulomb phase which does not contribute to the ELC or ECC density matrix. Inserting a complete set of partial waves in (27) leads to

$$\frac{d\sigma}{d\mathbf{v}}=\sum_{l,m,l'm'}(-1)^{l+l'}Y^m_l(\hat{\mathbf{v}})[Y^{m'}_l(\hat{\mathbf{v}})]^*\times\langle vlm\,|\,\sigma\,|\,vl'm'\rangle\delta_{m,m'} , \tag{30}$$

where $\langle vlm\,|\,\sigma\,|\,vl'm\rangle$ denotes the partial-wave density matrix which again is diagonal in m because of axial symmetry. The phase factor reflects the incoming boundary condition for the continuum wave. With the help of the addition theorem for spherical harmonics,[23] Eq. (30) can be cast into the form

$$\frac{d\sigma}{d\mathbf{v}}=\frac{1}{4\pi}\sum_{k=0}^{\infty}(2k+1)P_k(\cos\theta)\sum_{l,l',m}[(2l+1)(2l'+1)]^{1/2}\times(-1)^{l+l'-m}\begin{pmatrix}l&k&l'\\-m&0&m\end{pmatrix}\begin{pmatrix}l&k&l'\\0&0&0\end{pmatrix}\langle vlm\,|\,\sigma\,|\,vl'm\rangle . \tag{31}$$

In analogy to (12) we may define spherical state multipoles for continuum excitation,

$$\rho^k_q(l,l')=\sum_{m,m'}(-1)^{l-m}\sqrt{2k+1}\begin{pmatrix}l&k&l'\\-m&q&m\end{pmatrix}\langle vlm\,|\,\sigma\,|\,vl'm'\rangle . \tag{32}$$

Inserting (32) in (31) yields

$$\frac{d\sigma}{d\mathbf{v}}=\frac{1}{4\pi}\sum_{k=0}^{\infty}\sqrt{2k+1}P_k(\cos\theta)(-1)^k\sum_{l,l'}(-1)^l[(2l+1)(2l'+1)]^{1/2}\begin{pmatrix}l & k & l'\\ 0 & 0 & 0\end{pmatrix}\rho_0^k(l,l') . \tag{33}$$

Equation (33) can be further simplified by introducing statistical multipoles for continuum excitation similar to Eq. (11),

$$\sigma_0^k(v,\Pi,k,0)=(-1)^k(2-\delta_{k,0})^{1/2}\sum_{l,l'=0}^{\infty}(-1)^l\sqrt{(2l+1)(2l'+1)}\begin{pmatrix}l & k & l'\\ 0 & 0 & 0\end{pmatrix}\rho_0^k(l,l') , \tag{34}$$

to give

$$\frac{d\sigma}{d\mathbf{v}}=\frac{1}{4\pi}\sum_{k=0}^{\infty}\left[\frac{2k+1}{2-\delta_{k,0}}\right]^{1/2}\sigma_0^k(v,\Pi,k,0)P_k(\cos\theta) . \tag{35}$$

Here, as in Eq. (11), we have explicitly displayed the v dependence of σ_0^k. By comparing (35) and (27), the expansion coefficients of the DDCS can be expressed in terms of statistical multipoles as

$$\sigma_0=\lim_{v\to 0}\left[\frac{v}{4\pi}\sigma_0^0(v,0,0,0)\right] , \tag{36a}$$

$$\beta_k=\lim_{v\to 0}\left[\frac{2k+1}{2-\delta_{k,0}}\right]^{1/2}\sigma_0^k(v,\Pi,k,0)/\sigma_0^0(v,0,0,0) . \tag{36b}$$

Obviously, the statistical multipoles for Rydberg bound states [Eq. (19)] and for low-energy continuum states [Eq. (34)] are related to each other by continuity across the ionization limit. The continuity of the density matrix implies

$$\lim_{n\to\infty}[D(n)\langle nlm\mid\sigma\mid nl'm\rangle]=\lim_{v\to 0}[D(v)\langle vlm\mid\sigma\mid vl'm\rangle], \tag{37}$$

where

$$D(n)=n^3/Z_P^2 \tag{38a}$$

and

$$D(v)=v \tag{38b}$$

denote the density of states of given angular momentum (lm) below and above threshold, respectively. With Eqs. (19), (34), and (37) we find

$$\lim_{v\to 0}\sigma_0^k(v,\Pi,k,0)=\lim_{n\to\infty}\left[\frac{n^4}{vZ_P^2}\sigma_0^0(n,\Pi,k,0)\right] , \tag{39}$$

and consequently

$$\sigma_0=\lim_{n\to\infty}\left[\frac{n^4}{4\pi Z_P^2}\sigma(n,0,0,0)\right] \tag{40a}$$

and

$$\beta_k=\lim_{n\to\infty}\left[\frac{2k+1}{2-\delta_{k,0}}\right]^{1/2}\sigma_0^k(n,\Pi,k,0)/\sigma_0^0(n,0,0,0) . \tag{40b}$$

For later reference we remark that Eq. (40) together with the definition of $\sigma_0^k(n,\Pi,k,0)$ for finite n [Eq. (11)] permits a continuation of the "angular distribution" coefficients, $\beta_k(n)$, into the range of bound states with finite n. Equation (36) and (40) is the desired parametrization of the cusp cross section in terms of O(4) multipoles. Several interesting physical implications are worth mentioning.

(a) The DDCS for cusp electron emission can be calculated by taking the Rydberg limit of certain bound-state multipoles. An illustrative example will be discussed in the next section.

(b) Cusp multipoles and Rydberg multipoles possess a common physical interpretation in terms of multipoles of the RL vector. According to Eqs. (22) and (40) we have

$$\beta_k(n=\infty)=\left[-\frac{1}{Z_P}\right]^k(2k+1)\langle A_0^k\rangle . \tag{41}$$

It is crucial that the Runge-Lenz vector as a constant of motion has a well-defined meaning over the whole spectrum and facilitates a unified interpretation of anisotropic excitation above and below threshold. The usual picture of velocity anisotropy has no obvious meaning for bound states, at least for low-lying states for which a semiclassical description ceases to be valid. Conversely, electrostatic multipoles of the bound-state charge cloud frequently used to interpret bound state coherences[24,25] diverge in the Rydberg limit and for continuum manifolds. Their use would require appropriate renormalization on a case-by-case basis. For the dipole moment, the renormalization factor will be given below [Eq. (44)]. The obvious advantage of the multipole set A_0^k is that all expectation values remain finite over the whole spectrum owing to finite eigenvalues of $\mathbf{A}$.

(c) The cusp asymmetry parameter, β_1, which plays a major role in unraveling second-Born effects in ECC processes[26,27] can be related to the dipole moment of a bound state. The dipole operator ($\mathbf{d}$) and the Runge-Lenz vector are related to each other for a given n shell by[28]

$$\mathbf{d}=\frac{3}{2}\left[\frac{n}{Z_P}\right]^2\mathbf{A} . \tag{42}$$

Taking the expectation value for an axially symmetric matrix yields

$$\langle d_z\rangle=\frac{3}{2}\left[\frac{n}{Z_P}\right]^2\langle A_0^1\rangle . \tag{43}$$

With the aid of Eqs. (20) and (40) [recall that Eq. (20) is exact for arbitrary n in case $k=1$] $\langle d_z\rangle$ can be expressed in terms of $\beta_1(n)$ for bound states of principal quantum number n as

$$\langle d_z \rangle = -\frac{n}{2Z_P}(n^2-1)^{1/2}\beta_1(n) \ . \tag{44}$$

A cusp skewed to the low-velocity side, $\beta_1(n \cong \infty) < 0$, implies a positive dipole moment in Rydberg manifolds, i.e., the electron lags behind the projectile as expected. For $n \to \infty$ the dipole moment diverges quadratically. As mentioned above, a renormalized finite dipole moment can be defined by $\langle \tilde{d}_z \rangle = \langle d_z \rangle / n(n^2-1)^{1/2}$. A numerical application of (44) will be discussed in the next section.

V. THE n DEPENDENCE OF O(4) MULTIPOLES

We investigate the n dependence of the statistical O(4) multipoles for the electron capture process

$$H^+ + H(1s) \to H(n) + H^+ \tag{45}$$

at $v_P = 2$ a.u. using the continuum distorted-wave (CDW) approximation.[13]

The CDW approximation has the attractive features that it treats the distortion in the entrance and exit channel symmetrically and provides the T matrix element in analytical form for arbitrary hydrogenic final states (nlm).[29] Recent investigations have displayed, however, several conceptually unsatisfactory features of the CDW approximation. Among these are a "dip" in the differential capture cross section at the critical angle θ_T for Thomas double scattering,[30] an order of magnitude overestimate of the capture cross section into Rydberg states[31] with large angular momenta $l \gtrsim 1$, and the lack of certain on-shell portions of the double-scattering contribution.[32] While the CDW results are not expected to be accurate, its relatively simple analytical structure permits a systematic investigation of the n dependence of the density matrix over a wide range of n. Our numerical results serve primarily illustrative purposes. Nevertheless, many of the conclusions regarding the observed n systematics are expected to be valid despite the shortcomings of the CDW approximation.

Figure 3 depicts the behavior of the three low-order multipoles σ_0, β_1, and β_2 as a function of n^{-2} (the binding energy). The threshold values [Eq. (40)] are accordingly given by the points where the extrapolated curves intersect with the ordinate. Higher-order multipoles ($k > 2$) are generally small for ECC. The convergence as a function of the number of l substates (or, partial waves in the continuum) is displayed by indicating partial sums for the statistical multipoles [Eq. (11)] including angular momentum states up to a certain l value. The convergence is slower the higher the rank of the multipole, as expected. From Eqs. (21), (38), and (39) it can be easily seen that the Oppenheimer n^{-3} rule[33] for the shell capture cross section would correspond to a constant σ_0 as a function of the final-state binding energy. The small but finite slope indicates deviations from an exact n^{-3} behavior for finite n which is not surprising at relatively low velocities. The actual value of the slope might be, in addition, slightly exaggerated by the CDW approximation since cross sections for higher l states (and increasing statistical weight) are generally overestimated.[31] The finite value at threshold indicates, however, that the n^{-3} rule becomes valid for asymptotically high n.

The leading anisotropy parameter, $\beta_1(n)$, describing the forward-backward asymmetry of the charge cloud is remarkably insensitive with respect to variation in the binding energy, in full agreement with a smooth behavior of the density matrix along a Rydberg series. This can be exploited to determine the dipole moment of a collisionally formed Rydberg atom for arbitrary n to a very good degree of approximation by simple interpolation. Equation (44) gives the dipole moment as a product of a strongly n dependent but purely geometrical factor $[-n(n^2-1)^{1/2}/(2Z_P)]$ times $\beta_1(n)$, which contains all the dynamical aspects of the excitation process but is almost n independent. For $H(n \cong 100)$, for instance, the CDW approximation predicts a value $\beta_1 \cong 0.32$ and therefore a dipole moment of $\langle d_z \rangle \cong 1570$ a.u. corresponding to an electron lagging behind the proton by about 830 Å. Experimental data[34–36] indicate that $\beta_1(n)$ and therefore the dipole moment is even larger. While the CDW approximation very likely underestimates the value of $\beta_1(n)$, the weak n dependence and the simple interpolation procedure should be valid for a more advanced charge transfer theory like the distorted-wave Born (DWB) approximation.[37]

The convergence behavior of β_2 as a function of included l substates displays directly the influence of different

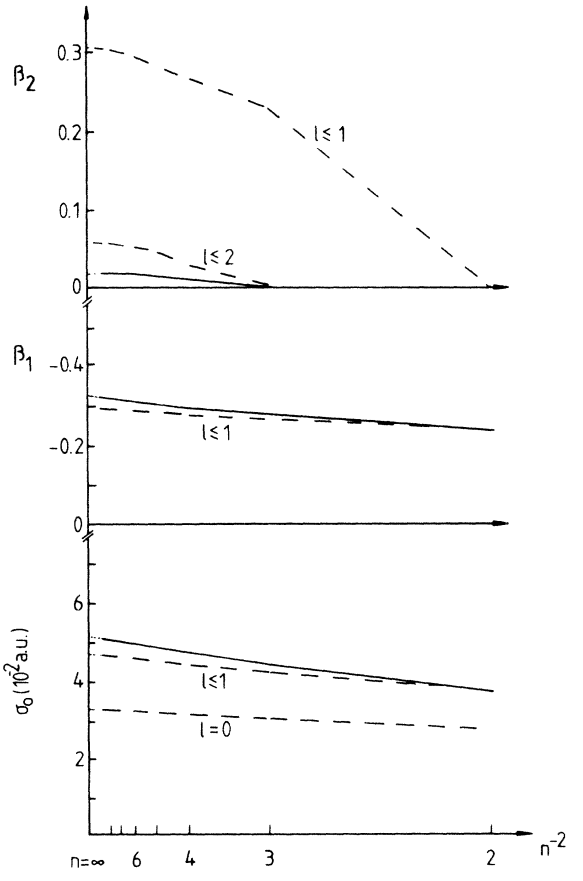

FIG. 3. Statistical multiples σ_0, β_1, and β_2 as a function of n^{-2} (binding energy of final state) for $H^+ + H(1s) \to H(n) + H^+$ ($v_P = 2$ a.u.) in CDW approximation. ——, sum over all l states; — — —, partial sums.

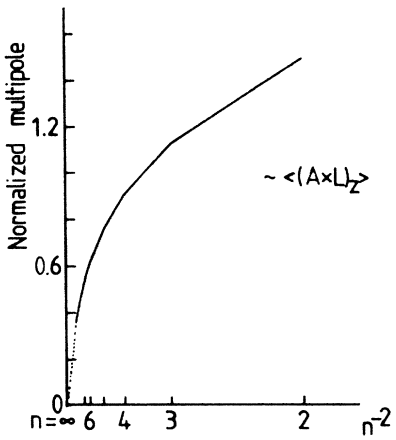

FIG. 4. n dependence of $\sqrt{3/2}\sigma_0^1(1,1,1)/\sigma_0^0(0,0,0)$ for $H^+ + H(1s) \rightarrow H(n) + H^+$ ($v_P = 2$ a.u.) in CDW approximation. This multipole is proportional to $\langle (\mathbf{A} \times \mathbf{L})_z \rangle$.

types of coherences. If $l \leqq 1$, according to the Wigner-Eckart theorem[23] β_2 is proportional to the Fano-Macek p-state alignment. If, in addition, d states are included ($l \leqq 2$) a different type of coherence of tensorial rank 2, the s-d coherence first observed in beam-foil spectroscopy[38] interferes destructively with the p-state alignment yielding a largely reduced β_2. Similar interferences occur for higher l states. As a result, β_2 is, except for lower velocities, quite small. As discussed in Sec. III, O(4) multipoles odd under time reversal vanish in the limit $n \rightarrow \infty$ provided only low-l states are populated. A numerical example for the approach of this limit is presented in Fig. 4. The multipole

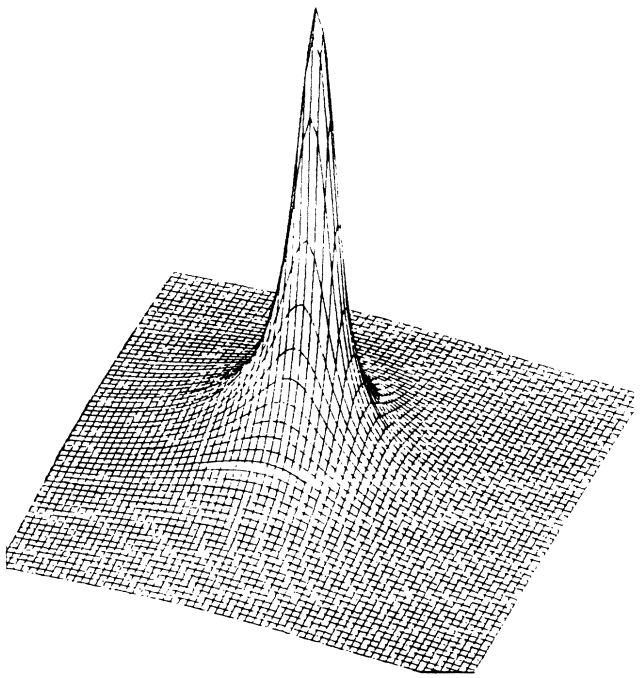

FIG. 5. Normalized velocity distribution for ECC $H^+ + H(1s) \rightarrow (H^+ + e^-) + H^+$ in CDW approximation ($v_P = 2$ a.u.) convoluted with an energy resolution $\delta E = 0.5\%$ and angular resolution $\Delta\theta = 0.2°$ ($-0.2 \leqq v_{||}, v_\perp \leqq 0.2$).

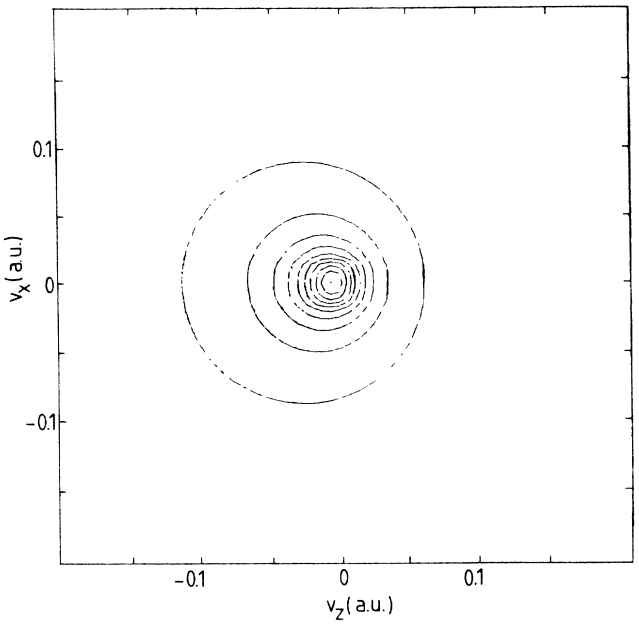

FIG. 6. Contour lines for the ECC distribution (see Fig. 5). Neighboring contours correspond to an increase by 0.1 times the peak height.

$$\sqrt{3/2}\sigma_0^1(n,1,1,1)/\sigma_0^0(n,0,0,0) \sim \langle (\mathbf{A} \times \mathbf{L})_z \rangle$$

dominates for low n states[35] over β_1. It monotonically decreases as $n \rightarrow \infty$, approaching zero in the Rydberg limit.

The post-collision interaction (PCI) correction,[39] taking into account long-range Stark mixing of the excited-state manifold in the exit channel, plays a minor role for leading multipoles σ_0 and β_k. This follows from the fact that the linear Stark operator $-d_z F = 3Fn^2 A_z / 2Z_P^2$ commutes with A_0^k in the Rydberg limit. This is linked to the well-known contraction[28] of the dynamical symmetry group $O(4) \rightarrow E(3)$ at threshold. The PCI correction is therefore omitted.

The Rydberg limit of σ_0, β_1, and β_2 determine according to Eqs. (34) and (35) the cusp cross section shown in Fig. 5. The contour lines (Fig. 6) clearly exhibit the velocity asymmetry with a preferred emission in the backward direction linked to the dipole moment discussed above through the same expectation value $\langle A_z \rangle$. We note that previous calculations[40,41] for ionization using a CDW approximation and a projectile-centered continuum wave function did not provide detailed information on the cusp shape.

VI. VELOCITY DEPENDENCE OF ECC SHAPE PARAMETER

In this section we study the multipole parameter for the ECC cusp for the charge transfer process

$$H^+ + He \rightarrow (H^+ + e^-) + He^+ \tag{46}$$

as a function of the projectile velocity using the CDW approximation together with a Hartree-Fock wave function[42] for the He($1s$) ground state.

In Fig. 7 we compare experimental data for the monopole term $\sigma_c = 4\pi\sigma_0$ with the CDW approximation. The

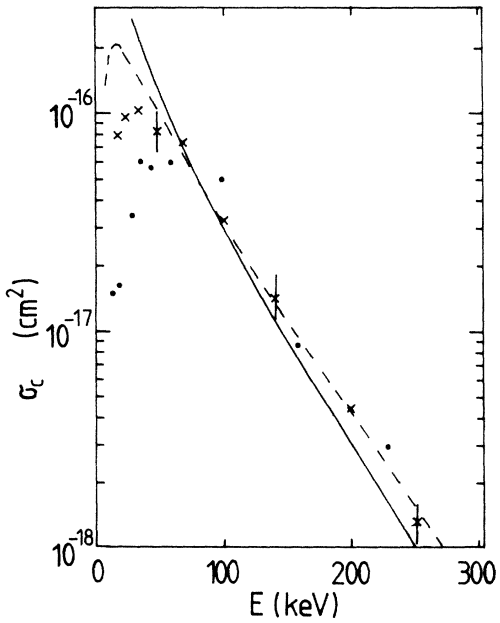

FIG. 7. Monopole term $\sigma_c = 4\pi\sigma_0$ of the cusp cross section as a function of the projectile energy for ECC: $H^+ + He \rightarrow (H^+ + e^-) + He^+$; ●, Rødbro and Andersen (Ref. 44); ×, Dahl (Ref. 45); — — —, Barnett *et al.* (Ref. 43); ——, CDW.

dashed line represents experimental data for total bound-state cross section converted into σ_c using Eq. (40) and an n^{-3} rule for excited-state cross sections.[43–45] The agreement between the CDW calculation and the data above 100 keV ($v_P = 2$ a.u.) is reasonably good, while at lower energies the lack of normalization of the CDW wave[46] leads to a systematic overestimate.

In Fig. 8 we compare various experimental[12,34,36,44,45] and theoretical[21,35] results for the dipole β_1 for both *continuum-state and bound-state* excitation. A direct quantitative comparison of these seemingly different measurements becomes possible when expressed in terms of the common expectation value $\langle A_z \rangle$. We note the good agreement between the cusp data ($n \rightarrow \infty$) of Andersen *et al.*[36] and Dahl[45] with bound-state dipole data ($n = 3$) of Havener *et al.*,[34] supporting our conjecture of a weak n dependence of $\beta_1(n)$. The experimental data of Meckbach *et al.*[12] are in disagreement with all other data. The source of this discrepancy is not yet known. The weak n dependence over a wide range of projectile velocities is also displayed by the CDW results for $n = 3$ and $n = \infty$.

While CDW approximation reproduces the v_P dependence of data better than the asymptotic second Born (B2) approximation,[21] the magnitude of $\beta_1(n)$ is systematically too small. At higher velocities, the impulse approximation[21] (IA—post form) seems to be in better agreement. However, since the post form of the IA is valid only for asymmetric systems with the projectile assumed to provide the stronger of the two potentials the agreement for proton-helium scattering might be fortuitous. We note that in a recent calculation using an extended VPS approximation,[47] nonvanishing values for β_1 have been found only when the internuclear potential was included. This is inconsistent with the fact that angle-integral cross sections[48] as well as coherence parameters[49] should be independent of the internuclear potential [up to corrections of the order of (electron mass/nucleus mass)]. The v_P dependence of the quadrupole moment β_2 of the cusp electron distribution as predicted by the CDW approximation is displayed in Fig. 9. Experimental data for comparison are presently not available, except for the observation[50] that for other systems β_2 is relatively small in qualitative agreement with Fig. 9.

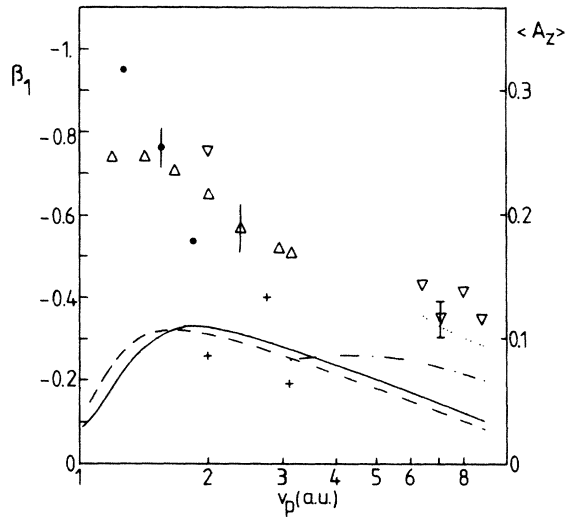

FIG. 8. Dipole term β_1 for $H^+ + He \rightarrow H(n) + He^+$ as a function of projectile velocity; ●, Havener *et al.* (Ref. 34) ($n = 3$); ∇, Andersen *et al.* (Ref. 36) ($n = \infty$); Δ, Dahl (Ref. 45) ($n = \infty$); +, Meckbach *et al.* (Ref. 12) ($n = \infty$); —·—·—, asymptotic B_2 approximation (Ref. 21) ($n = \infty$); · · · ·, IA (Ref. 21) ($n = \infty$); — — —, CDW (Ref. 35) ($n = 3$); ——, CDW ($n = \infty$).

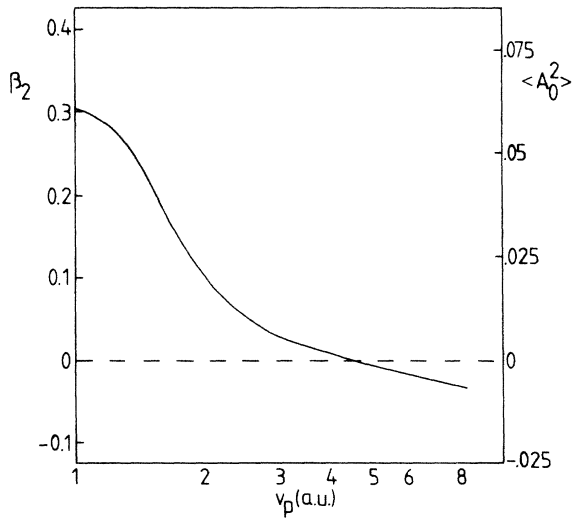

FIG. 9. Quadrupole term β_2 for $H^+ + He \rightarrow (H^+ + e^-) + He^+$ as a function of the projectile velocity in CDW approximation.

VII. CONCLUDING REMARKS

We have introduced a unified description of anisotropies for near-threshold excitation in a Coulomb field in terms of statistical O(4) multipoles. It has been shown that a common set of parameters, the multipoles of the Runge-Lenz vector **A**, can represent both the multipoles of the velocity distribution in the low-energy continuum and of the charge cloud distribution in Rydberg manifolds. Calculations employing the CDW approximation have displayed a remarkable smooth n dependence of these statistical multipoles.

Several future applications may be envisioned: Experimental data and the CDW approximation show a large ECC cusp forward-backward asymmetry. Smooth extrapolation of β_1 predicts a large dipole moment in Rydberg orbits produced by electron capture. This dipole moment should be experimentally observable as a directional dependence in the field ionization of Rydberg electrons produced in charge transfer collisions.

In the medium—to—high-energy range coupled-channel calculations are most reliable. They are, however, difficult to apply to cusp electron emission, because of inherent difficulties, to adequately represent the near-threshold continuum. The smooth n dependence of the O(4) multipoles suggests a practical method to circumvent this problem. Calculation of statistical multipoles for a few medium n states (above the most probable n shell) within a coupled-channel code and smooth extrapolation to threshold should suffice to reliably estimate the cusp cross section.

In this paper we have applied the description of coherent Rydberg-state excitation in terms of O(4) variables to hydrogen whose nonrelativistic Hamiltonian possesses the O(4) supersymmetry. Formally, this description may be generalized to nonhydrogenic systems. Since the O(4) variables form a complete set for the n-shell density matrix, this set can also be used to describe coherent one-electron excitation in nonhydrogenic systems (e.g., alkali atoms). However, its specific intuitive significance compared to any other complete basis sets depends on the Hamiltonian of the atomic subsystem under investigation. For Rydberg series with small but finite quantum defects or relativistic corrections, **A** is no longer a constant of motion but precesses with frequencies given by the energy splittings within an n shell. The present description of the collisionally prepared density matrix is therefore expected to be meaningful as long as the collision time is short compared with the inverse precession frequency.

ACKNOWLEDGMENTS

I would like to thank L. Andersen, S. Berry, L. Dubé, I. Sellin, and K. Taulbjerg for many valuable discussions. This research was supported by the National Science Foundation; by the U.S. Department of Energy, under Contract No. DE-AC05-84OR21400 with Martin Marietta Energy Systems, Inc; and by the Deutsche Forschungsgemeinschaft (Sonderforschungsbereich 161), FU Berlin, Germany.

[1]C. B. Crooks and M. E. Rudd, Phys. Rev. Lett. **25**, 1599 (1970); K. G. Harrison and M. W. Lucas, Phys. Lett. **33A**, 142 (1970).

[2]For a review, see V. H. Ponce and W. Meckbach, Comments At. Mol. Phys. **10**, 231 (1981); M. Breinig *et al.*, Phys. Rev. A **25**, 3015 (1982); K. O. Groeneveld, W. Meckbach, I. A. Sellin, and J. Burgdörfer, Comments At. Mol. Phys. **14**, 187 (1984).

[3]J. Macek, Phys. Rev. A **1**, 235 (1970); M. Lucas, W. Steckelmacher, J. Macek, and J. Potter, J. Phys. B **13**, 4833 (1980).

[4]M. E. Rudd and J. Macek, Case Stud. At. Mol. Phys. **3**, 47 (1972).

[5]W. Meckbach, R. Vidal, P. Focke, I. B. Nemirovsky, and C. E. Gonzalez-Lepera, Phys. Rev. Lett. **52**, 621 (1984).

[6]S. B. Elston *et al.*, in *Forward Electron Ejection in Ion Collisions,* Vol. 213 of *Lecture Notes in Physics,* edited by K. O. Groeneveld, W. Meckbach, and I. A. Sellin (Springer, Berlin, 1984), p. 75.

[7]E. Kanter, D. Schneider, Z. Vager, D. Gemmell, B. Zabransky, G. Yuanzhuang, P. Arcuni, P. Koch, D. Mariani, and W. Van de Water, Phys. Rev. A **29**, 583 (1984); P. Engar, M. Breinig, R. DeSerio, C. E. Gonzalez-Lepera, and I. A. Sellin (unpublished).

[8]H. D. Betz, D. Röschenthaler, and J. Rothermel, Phys. Rev. Lett. **50**, 34 (1983).

[9]D. Schneider, W. Zeitz, G. Schiewitz, and N. Stolterfoht, in *Abstracts of the Fourteenth International Conference on the Physics of Electronic and Atomic Collisions, Palo Alto, 1985,* edited by M. J. Coggiola, D. L. Huestis, and R. P. Saxon (ICPEAC, Palo Alto, 1985), p. 634.

[10]E. P. Wigner, Phys. Rev. **73**, 1002 (1948).

[11]J. Burgdörfer, Z. Phys. A **309**, 285 (1983). We take the opportunity to correct a misprint in a phase factor in Eq. (36) of this reference. The correct form is given in Eq. (11) of the present paper.

[12]W. Meckbach, I. B. Nemirovsky, and C. Garibotti, Phys. Rev. A **24**, 1793 (1981).

[13]I. M. Cheshire, Proc. Phys. Soc. London **84**, 89 (1964).

[14]K. Blum, *Density Matrix Theory and Applications* (Plenum, New York, 1981).

[15]H. Gabriel and J. Bosse, in *Proceedings of the International Conference on Angular Correlations in Nuclear Disintegration, Delft, 1970,* edited by H. van Krugten and B. van Nooijen (Rotterdam University Press, Groningen, 1971), p. 394ff.

[16]The definition of U_q^k in Eq. (6) differs from the definition of V_q^k in Ref. 22, Eq. (27), by the constant required to satisfy the normalization condition [Eq. (9)]. Unfortunately, various definitions are in use for the spherical tensor components J_q^k of an angular momentum **J** which differ from each other by q-independent factors. Here, we adopt the definition of Ref. 19 which seems to be widely accepted.

[17]We note that the recently observed selective laser excitation of "circular" Rydberg states can reach much higher l values; see R. Hulet and D. Kleppner, Phys. Rev. Lett **51**, 1430 (1983).

[18]J. Burgdörfer (unpublished).

[19]D. Smith and J. H. Thornley, Proc. Phys. Soc. London **89**, 779 (1966).

[20]U. Fano and J. Macek, Rev. Mod. Phys. **43**, 553 (1973).

[21]D. Jakubassa-Amundsen, in Ref. 6, p. 17.

[22]J. Burgdörfer, in Ref. 6, p. 32.
[23]D. Brink and G. Satchler, *Angular Momentum* (Clarendon, Oxford, 1968).
[24]I. A. Sellin, J. R. Mowat, R. S. Peterson, P. M. Griffin, R. Laubert, and H. Haselton, Phys. Rev. Lett. **31**, 1335 (1973); A. Gaupp, H. J. Andrä, and J. Macek, *ibid.* **32**, 268 (1974).
[25]C. C. Havener, N. Rouze, W. B. Westerveld, and J. S. Risley, Phys. Rev. A **33**, 276 (1986).
[26]R. Shakeshaft and L. Spruch, Phys. Rev. Lett. **41**, 1037 (1978).
[27]M. Breinig *et al.*, Phys. Rev. Lett. **45**, 1689 (1980).
[28]M. Englefield, *Group Theory and the Coulomb Problem* (Wiley-Interscience, New York, 1972).
[29]L. J. Dubé, J. Phys. B **17**, 641 (1984).
[30]R. Rivarola and J. Miraglia, J. Phys. B **15**, 2221 (1982).
[31]J. Burgdörfer and L. Dubé, Phys. Rev. A **31**, 634 (1985).
[32]J. Burgdörfer and K. Taulbjerg, Phys. Rev. A (to be published).
[33]J. R. Oppenheimer, Phys. Rev. **31**, 349 (1928).
[34]C. C. Havener, W. B. Westerveld, J. Risley, N. Tolk, and J. C. Tully, Phys. Rev. Lett. **48**, 926 (1982).
[35]J. Burgdörfer and L. Dubé, Phys. Rev. Lett. **52**, 2225 (1984).
[36]L. Andersen, K. Jensen, and H. Knudsen (unpublished).
[37]K. Taulbjerg, in *Fundamental Processes in Energetic Atomic Collisions,* NATO Advanced Study Series 1, edited by H. O. Lutz, J. S. Briggs, and H. Kleinpoppen (Plenum, New York, 1983), p. 349.
[38]D. Burns and W. Hancock, Phys. Rev. Lett. **27**, 379 (1970).
[39]J. Burgdörfer, Phys. Rev. A **24**, 1756 (1981).
[40]D. Belkić, J. Phys. B **11**, 3529 (1978).
[41]D. S. F. Crothers and J. F. McCann, J. Phys. B **16**, 3229 (1983).
[42]E. Clementi and C. Roetti, At. Nucl. Data **14**, 185 (1974).
[43]F. J. de Heer, J. Schutten, and H. Moustoffa, Physica **32**, 1766 (1966).
[44]M. Rødbrø and F. Andersen, J. Phys. B **12**, 2883 (1979).
[45]P. Dahl, J. Phys. B **18**, 1178 (1985).
[46]D. S. F. Crothers, J. Phys. B **15**, 2061 (1982).
[47]R. Barrachina and C. R. Garibotti, Phys. Rev. A **28**, 1821 (1983).
[48]J. D. Jackson and H. Schiff, Phys. Rev. **89**, 359 (1953).
[49]J. Burgdörfer, J. Phys. B **14**, 1019 (1981).
[50]S. Berry *et al.*, Phys. Rev. A **31**, 1392 (1985).